Lipid accumulation of *Chlorella* sp. TLD6B from the Taklimakan Desert under salt stress

Hong Li [1], **Jun Tan** [2], **Yun Mu** [2], **Jianfeng Gao** [Corresp. 2]

[1] College of Life Sciences; Key Laboratory of Xinjiang Phytomedicine Resource and Utilization, Ministry of Education, School of Pharmacy, Shihezi University, Shihezi, Xinjiang, China

[2] College of Life Sciences, Shihezi University, Shihezi, Xinjiang, China

Corresponding Author: Jianfeng Gao
Email address: jianfengg@shzu.edu.cn

Chlorella has become an important raw material for biodiesel production in recent years, and *Chlorella* sp. TLD6B, a species with high lipid concentrations and high salt and drought tolerance, has been cultivated on a large scale. To explore the lipid accumulation of *Chlorella* sp. TLD6B and its relationship to external NaCl concentrations, we performed physiological measurements and genome-wide gene expression profiling under different levels of salt stress. *Chlorella* sp. TLD6B was able to tolerate high levels of salt stress (0.8 M NaCl addition). Lipid concentrations initially increased and then decreased as salt stress increased and were highest under the addition of 0.2 M NaCl. Comparative transcriptomic analysis revealed that salt stress enhanced the expression of genes related to sugar metabolism and fatty acid biosynthesis (the *ACCases BC* and *BCCP*, *KAS II*, and *GPDHs* involved in TAG synthesis), thereby promoting lipid accumulation under the addition of 0.2 M NaCl. However, high salinity inhibited cell growth. Expression of three *SADs*, whose encoded products function in unsaturated fatty acid biosynthesis, was up-regulated under high salinity (0.8 M NaCl addition). This research clarifies the relationship between salt tolerance and lipid accumulation and promotes the utilization of *Chlorella* sp. TLD6B.

1 **Lipid accumulation of *Chlorella* sp. TLD6B from the Taklimakan Desert**
2 **under salt stress**

3 Hong Li[1,2], Jun Tan[1], Yun Mu[1], Jianfeng Gao[1,*]
4 [1]College of Life Sciences, Shihezi University, Shihezi, Xinjiang, China
5 [2]Key Laboratory of Xinjiang Phytomedicine Resource and Utilization, Ministry of Education, School of
6 Pharmacy, Shihezi University, Shehezi, Xinjiang 832003, China
7 [*]Corresponding author.
8
9 Corresponding Author:
10 Jianfeng Gao[1]
11 Beisi Road, Shihezi, Xinjiang, 832000, China
12 Email address: jianfengg@shzu.edu.cn

Abstract

15 *Chlorella* has become an important raw material for biodiesel production in recent years, and
16 *Chlorella* sp. TLD6B, a species with high lipid concentrations and high salt and drought
17 tolerance, has been cultivated on a large scale. To explore the lipid accumulation of *Chlorella* sp.
18 TLD6B and its relationship to external NaCl concentrations, we performed physiological
19 measurements and genome-wide gene expression profiling under different levels of salt stress.
20 *Chlorella* sp. TLD6B was able to tolerate high levels of salt stress (0.8 M NaCl addition). Lipid
21 concentrations initially increased and then decreased as salt stress increased and were highest
22 under the addition of 0.2 M NaCl. Comparative transcriptomic analysis revealed that salt stress
23 enhanced the expression of genes related to sugar metabolism and fatty acid biosynthesis (the
24 *ACCases BC* and *BCCP*, *KAS II*, and *GPDHs* involved in TAG synthesis), thereby promoting
25 lipid accumulation under the addition of 0.2 M NaCl. However, high salinity inhibited cell
26 growth. Expression of three *SADs*, whose encoded products function in unsaturated fatty acid
27 biosynthesis, was up-regulated under high salinity (0.8 M NaCl addition). This research clarifies
28 the relationship between salt tolerance and lipid accumulation and promotes the utilization of
29 *Chlorella* sp. TLD6B.

30 **Subjects:Agricultural and Biological Sciences, Microbiology, Plant Science**

31 **Keywords:** Salt stress, *Chlorella* sp. TLD6B, Transcriptome, Lipid accumulation

INTRODUCTION

34 Increasing global energy demands cause over-exploitation and shortages of nonrenewable
35 resources such as oil, natural gas, and coal and increase the urgency associated with research on
36 bioenergy. As photoautotrophic organisms (*Schenk et al., 2008*), microalgae are characterized by
37 high lipid concentrations and rapid growth, which makes them the most promising organisms for
38 the development of biodiesel (*Halim et al., 2012*). The lipid metabolism of microalgae is a

39 complex process that involves the synthesis and metabolism of fatty acids, triglycerides (TAGs),
40 acetyl-CoA, and other compounds, and it is closely related to algal growth and stress tolerance
41 (*Gao et al., 2014*). Environmental changes alter the expression of many genes encoding enzymes
42 in these metabolic pathways and thereby influence microalgal lipid metabolism. Previous studies
43 have found that lipid accumulation in microalgae is affected by changes in the expression of the
44 ACCase subunit genes *BC*, *BCCP*, and *α-CT*, the fatty acid synthesis genes *SAD*, *KAS II*, *MCAT*,
45 as well as the TAG synthesis genes *GPAT*, *PAP*, *LPATT*, and *DGAT* (*Zalutskaya et al., 2015;*
46 *Huang et al., 2016*). At present, the detailed signaling mechanisms that regulate lipid metabolism
47 in microalgae remain unclear. However, lipid accumulation is known to be regulated by abscisic
48 acid (ABA) and reactive oxygen species (ROS) signals (*Gao et al., 2014; Wang et al., 2016*),
49 indicating that microalgal lipid metabolism is closely related to adaptation to unfavorable
50 environments.
51   *Chlorella* is a eukaryotic, single-celled green microalga that is widely distributed in fresh
52 water, soils, and deserts (*Li et al., 2016*). It has been widely used in research related to
53 microalgae energy production (*Liang et al., 2009; Li et al., 2011; Liu et al., 2011*). Researchers
54 currently focus primarily on freshwater *Chlorella*, and there have been few studies of desert
55 *Chlorella*. Desert *Chlorella* grows in an extremely arid environment, with a maximum
56 temperature of 67.2 °C in intense heat and a temperature difference of more than 40 °C between
57 day and night. The winter is cold, with low precipitation and high evaporation (*Zhang et al.,*
58 *2020*). Lewis and Flechtner *(2002)* found that desert green algae evolved from aquatic green
59 algae at least five independent times. Therefore, desert *Chlorella* has adapted to the extremely
60 harsh arid environment, making it an excellent material for studying the molecular biology of
61 stress resistance at the single-cell level (*Mu et al., 2016*). In the past, studies of desert algae have
62 focused mainly on the algal composition of microbiotic crusts and the characteristics and
63 functions of crust formation (*Ashley & Rushforth, 1984; Garcia-Pichel et al., 2001; Lewis &*
64 *Flechtner, 2002; Zhao et al., 2006*). In recent years, Li et al. (*2012*) and Wang et al. (*2014*)
65 analyzed the phylogeny of several strains of microalgae in the Gurbantonggut and Taklimakan
66 Deserts. Among these algae, GTD7c-2, TLD2A, TLD6B are classified as *Chlorella*. Gong et al.
67 (*2013*) compared different cultivation methods for desert *Chlorella* GTD8A1. Zhu et al. (*2014*)
68 and Mu et al. (*2016*) measured the oil content of desert microalgae and desert *Chlorella*,
69 respectively, and made a preliminary assessment of their potential for conversion to biodiesel.
70   Previous studies on lipid accumulation in freshwater *Chlorella* under salt stress have
71 provided useful information, but there have been no reports on the mechanisms of lipid
72 accumulation in desert *Chlorella* under salt stress. Desert *Chlorella* sp. TLD6B differs from
73 fresh water algae, as it grows in extremely harsh environments. We must first clarify the
74 mechanistic relationship between salinity stress and lipid accumulation before we can further
75 develop desert *Chlorella* sp. TLD6B for use in biofuel production. Studies have shown that lipid
76 accumulation in *Chlorella* can be induced by salt stress (*Wang et al., 2016*) and that salinity
77 enhances microalgal lipid accumulation for biofuel production (*BenMoussa-Dahmen et al.,*
78 *2016; Srivastava et al., 2017*). High salinity is an important factor that stimulates lipid

79 accumulation, but it also has adverse effects on biomass growth and lipid production in
80 microalgae (*Markou & Nerantzis, 2013; Ho et al., 2014*). Sharma and Chauhan (*2016*) used
81 comparative transcriptomics to identify the molecular components associated with differences in
82 lipid accumulation between the microalgal species *Scenedesmus dimorphus* and *S. quadricauda*.
83 Gao et al. (*2014*) used transcriptomics, genomics, and proteomics to characterize lipid
84 accumulation mechanisms of the oleaginous microalga *C. protothecoides*.
85   Here, we studied *Chlorella* sp. TLD6B, a desert *Chlorella* collected from the Taklimakan
86 Desert that exhibits greater drought and salt tolerance than freshwater *Chlorella* (unpublished
87 results). We investigated the mechanism of lipid accumulation in *Chlorella* sp. TLD6B under
88 salt stress by measuring relevant physiological parameters and analyzing whole-genome gene
89 expression profiles under different levels of salt stress. This research aims to clarify the
90 relationship between salt stress and oil accumulation in *Chlorella* sp. TLD6B and to promote its
91 development and utilization in biofuel production.

MATERIALS AND METHODS

Algal strain and culture conditions

94 The experimental algae were collected from the Taklimakan Desert (37°36' N, 80°23' E, 1254 m
95 altitude, 3.5 ℃ average surface temperature, 0.4 M average NaCl salt concentration, 71.2 W·m^{-2}
96 net radiation at 16:00) in Xinjiang Province, China. Field experiments were approved by the
97 College of Life Sciences of Shihezi University (project number: 2011-GB-200900-G). The algae
98 were isolated in the laboratory from a mixed culture of Taklimakan Desert soil samples and were
99 identified as *Chlorella* sp. TLD6B (*Wang et al., 2014*). They were maintained in an autotrophic
100 culture system at the College of Life Sciences, Shihezi University, China. Bold basal medium
101 (BBM; *Nichols, 1973*) was autoclaved, and algal cells in the logarithmic growth phase were
102 inoculated into Erlenmeyer flasks containing 500 mL BBM medium at a ratio of 20% (V/V). The
103 initial cell density was controlled at an OD_{680} of approximately 0.1, and the preparation of BBM
104 medium is described in Table S1. Light was provided by white fluorescent lamps at an intensity
105 of 72 μmol photons m^{-2} s^{-1} with a 12h/12h light-dark cycle, and the temperature was 23 ℃.
106 Flasks were shaken three times a day at regular intervals and cultured for 24 d (*Mu et al., 2016*).

Salt stress treatments

108 Algal cells in the logarithmic growth phase were inoculated into Erlenmeyer flasks containing
109 300 mL BBM medium, and 0.0, 0.1, 0.2, 0.4, 0.6, or 0.8 M NaCl was added to supplement the
110 medium to a final volume of 500 mL. The 0.0 NaCl treatment was the control, and there were
111 three replicates of each treatment. Algal culture was performed as described above. Samples
112 were obtained every 6 d after inoculation to measure physiological and biochemical indexes such
113 as biomass, carbohydrate concentration, and total lipid concentration.

Measurement of physiological and biochemical indexes

115 Culture solution (100 mL) was added to 10-mL centrifuge tubes at 4 ℃, and the tubes were

116 centrifuged at 8000 rpm for 15 min. The supernatant was discarded, and 2 mL of deionized water
117 was added. The cell sediments were washed three times by vortexing (5–10 s each time), then
118 divided into two equal parts. One part was used for dry weight measurement, and the other was
119 immediately frozen in liquid nitrogen and stored at −80 °C for further analysis.

120   Optical density at 680 nm (OD_{680}) was determined using a UV-5800H UV–VIS
121 spectrophotometer (Metash, Shanghai, China), and a growth curve was drawn (*Gong et al.,*
122 *2013*). The centrifuged *Chlorella* sp. TLD6B sediment was dried at 80 °C for 24 h to measure the
123 dry weight (*Wan et al., 2015*). The specific growth rate was calculated using the method of
124 Wang et al. *(2016)*.

125

126 $$\mu = \frac{\lg N_1 - \lg N_0}{t_1 - t_0} \times 3.322 \qquad (1)$$

127

128   Where μ is the specific growth rate, mg L^{-1} d^{-1}; N_0 is the biomass from the previous
129 sampling date, mg L^{-1}; N_1 is the current biomass, mg L^{-1}; and t_0 and t_1 are the culture times, $t_1 - t_0$
130 = 6 d.

131   The phenol-sulfuric acid method was used to measure carbohydrate content (*Dubois et al.,*
132 *1956*). The absorbance was measured at 490 nm on an iMark Microplate Reader (BIO-RAD,
133 USA). Different concentrations of glucose were used to create a standard curve (y = 8.55x−0.07,
134 where x is the standard concentration [μg mL^{-1}] and y is the absorbance value), from which the
135 glucose concentration X_C of the sample could be calculated. X_C (μg mL^{-1}) was defined as shown
136 in equation (Eq.) (2), and carbohydrate content (CC, %) was defined as shown in Eq. (3).

137

138 $$X_C = \frac{(\triangle A + 0.07)}{8.55} \qquad (2)$$

139

140 $$CC = \frac{X_C \times V \times 100\%}{V_C \times W} \qquad (3)$$

141

142   where $\triangle A$ is the absorbance at 490 nm, V is the total volume of the sample (mL), V_C is the
143 volume of the subsample used for measurement (μL), and W is the dry weight of the sample (g
144 L^{-1}).

145   The lipid content was measured by the colorimetric sulfo-phospho-vanillin method as
146 described by Mishra et al. (*2014*) with some modifications (*Li et al., 2012*). The absorbance was
147 measured at 528 nm, and the corresponding linoleic acid concentration (μg mL^{-1}) was calculated
148 from the standard curve (y = 0.0005x + 0.008). X_L (μg mL^{-1}) was defined as shown in Eq. (4), and
149 the lipid content (LC, %) was defined as shown in Eq. (5).

150

151 $$X_L = \frac{(\triangle A - 0.008)}{0.0005} \qquad (4)$$

152

153 $$LC = \frac{X_L \times V \times 100\%}{V_L \times W} \qquad (5)$$

154

155   where ΔA is the absorbance at 528 nm, V is the total volume of the extract (mL), V_L is the
156   volume of the subsample used for measurement (μL), and W is the dry weight of the sample (g
157   L^{-1}).

RNA extraction and sequencing

159   Based on the results of physiological measurements under salt stress, we selected *Chlorella* sp.
160   TLD6B cells grown under low salt stress (0.1 M NaCl addition) and high salt stress (0.8 M NaCl
161   addition) for 18 d for use in transcriptome sequencing and analysis. Samples collected from the
162   control group, the 0.1 M NaCl treatment group, and the 0.8 M NaCl treatment group were
163   labeled CK18, Nacl1, and Nacl2, respectively. Each treatment was replicated two times. Samples
164   were centrifuged at 8000 rpm for 8 min at 4 °C. After removal of the supernatants, *Chlorella* sp.
165   TLD6B cells were washed with distilled water three times and stored at −80 °C for RNA
166   extraction.
167   Total RNA was isolated from all samples using the TRIzol reagent (Invitrogen, USA)
168   according to the manufacturer's instructions. Total RNA was sent to Beijing Novogene
169   Technology Co., Ltd. for RNA quality assessment, library construction, and sequencing (150-bp
170   paired-end reads) on the Illumina NovaSeq 6000 platform. Raw sequence reads have been
171   deposited into the NCBI GEO under accession number GSE162916.

Transcriptome analysis

173   The total raw reads were processed using FASTQC software with default parameters. High-
174   quality clean reads were obtained by removing reads that contained adapters, reads that
175   contained more than 10% unknown nucleotides (N), and low-quality reads that contained more
176   than 50% low-quality bases ($Q_{phred} \leq 20$). At the same time, the GC content, Q20, Q30, and
177   sequence repetition level of the clean reads were calculated. Transcriptome *de novo* assembly
178   was performed using Trinity v2.4.0 software (*Grabherr et al., 2011*) with the parameter
179   Kmer = 25. Corset v1.05 (*Davidson & Oshlack, 2014*) was used with default parameters to
180   cluster the transcript sequences in order to remove redundant sequences and obtain unigene
181   sequence sets for subsequent analysis. The longest transcript of each subcomponent was used as
182   the unigene for functional annotation. All assembled unigenes were finally annotated by
183   comparing their sequences against the NR (NCBI non-redundant protein sequences, e-value =
184   10^{-5}), NT (NCBI nucleotide sequences, e-value = 10^{-5}), SwissProt (e-value = 10^{-5}), GO (Gene
185   Ontology, e-value = 10^{-6}), KEGG (Kyoto Encyclopedia of Genes and Genomes, e-value =
186   10^{-10}), PFAM (protein family, e-value = 0.01), and KOG/COG (euKaryotic Ortholog Groups/
187   Clusters of Orthologous Groups of Proteins, e-value = 10^{-3}) databases. For NR, SwissProt, and
188   KOG/COG annotations, Diamond v0.8.22 software was used. For NT annotation, Blastn (NCBI
189   blast 2.2.28+) was used. PFAM protein family alignments were performed using the HMMER
190   3.0 package. GO annotations were obtained based on the annotation results from NR and PFAM
191   using Blast2GO v2.5 software (*Götz et al., 2008*). The KEGG Automatic Annotation Server of
192   KAAS was used for KEGG pathway analysis. The clean reads were aligned to the Trinity

193   transcripts using Bowtie 2 with default parameters (*Langmead & Salzberg, 2012*). Following
194   alignment, raw read counts for each transcript were derived using RSEM v1.2.15 (*Li & Dewey,*
195   *2011*) with default parameters and then normalized to FPKM (Fragments Per Kilobase of
196   transcript per Million mapped reads) (*Trapnell et al., 2010*). The read counts were used as input
197   for the DESeq R package (1.10.1) (*Anders & Huber, 2010*) to identify differentially expressed
198   genes (DEGs) using the thresholds adjusted *P* value (padj) < 0.05 and |log$_2$ FoldChange| ≥ 1.
199   DEGs were mapped to terms in the GO and KEGG databases for functional and pathway
200   analysis. The GOseq R package (*Young et al., 2010*) was used for GO enrichment analysis, and
201   GO terms with corrected *P* value < 0.05 were defined as significantly enriched in the DEG set.
202   Significantly enriched KEGG pathways were identified in the DEGs using KOBAS v2.0.12 with
203   a corrected *P* value < 0.05 (*Mao et al., 2005*). The GO and KEGG enrichment maps were
204   generated using the Beijing Novogene Technology Co., Ltd. server. The two figures were
205   merged using Adobe Photoshop CS5 (Adobe Inc.; San Jose, CA, USA).

206   **Verification of RNA-seq gene expression by quantitative real-time PCR**

207   Samples of total RNA (3 µg) were taken from the same total RNA used for RNA sequencing and
208   used for the synthesis of first-strand cDNA with the M-MLV reverse transcription kit (Takara,
209   Japan) according to the manufacturer's instructions. The cDNA obtained by reverse transcription
210   was diluted 10-fold for use. Primer 5 software was used to design gene-specific real-time
211   quantitative PCR (qRT–PCR) primers. qRT–PCR was performed using the Roche Light Cycler
212   480 system (Roche, Rotkreuz, Switzerland) and the SYBR Premix ExTaq kit (Takara, Japan)
213   with a 10-µL PCR reaction system. The thermal cycle procedure was as follows: pre-incubation
214   at 95°C for 5 min, followed by 40 cycles of 95 °C for 15 s, 60 °C for 15 s, and 72 °C for 20 s.
215   The $2^{-\Delta\Delta Ct}$ method was used to calculate relative gene expression using the *GAPDH* gene as a
216   reference (*Livak & Schmittgen, 2001*). Pearson correlations between RNA-seq and qRT–PCR
217   expression fold changes were calculated using SPSS 20.0. Treatment differences were assessed
218   by analysis of variance using SPSS 20.0 (IBM Inc., Chicago, USA).

219   **Data analysis**

220   All physiological data are presented as the mean ± standard deviation of three replicates. SPSS
221   20.0 was used to perform one-way analysis of variance (ANOVA) and correlation analysis, and
222   Tukey's test was used to identify differences among individual treatments (*P* < 0.05).
223   Correlations between biomass and physiological indexes after different durations of salt stress
224   were obtained using the bivariate module in the correlate analysis tool of SPSS 20.0. Graphs
225   were constructed using SigmaPlot 12.5 software.

226   **RESULTS**

227   **Effects of different salt stress levels on the physiological characteristics of *Chlorella* sp.**
228   **TLD6B**

229   Biomass increased under low salt stress and decreased under high salt stress, and *Chlorella* sp.
230   TLD6B entered the logarithmic growth phase on the sixth day of culture. The OD$_{680}$

231 measurement increased rapidly before day 18, but slowed by day 24, entering a stable phase. The
232 OD_{680} measurement gradually decreased as the concentration of NaCl added to the medium
233 increased from 0.1 M to 0.8 M (Figure 1A and Table S2). The algae were able to tolerate high
234 levels of salt (0.6 M and 0.8 M NaCl addition), but their biomass was very low (Figure 1B and
235 Table S2). Biomass was higher in the 0.1 M and 0.2 M NaCl addition treatments than in the
236 control, but the OD_{680} measurement decreased with increasing NaCl concentrations in the
237 remaining treatments and also decreased with time. In general, compared with the control, the
238 0.1 M and 0.2 M NaCl addition treatments significantly inhibited the OD_{680} but increased
239 biomass. Biomass increased markedly after 12 days of NaCl stress in the 0.2 M NaCl addition
240 treatment, whereas addition of 0.4–0.8 M NaCl significantly inhibited both OD680 and biomass.

241   Carbohydrate content decreased as NaCl concentration increased: with the exception of the
242 0.2 M NaCl addition treatment, the higher the NaCl concentration in the culture solution, the
243 lower the algal carbohydrate content (Figure 1C and Table S2). However, lipid content and
244 biomass were improved by the addition of up to 0.2 M NaCl. Lipid content as a function of NaCl
245 concentration was directly proportional to algal biomass, and *Chlorella* sp. TLD6B exhibited the
246 highest lipid contents of 29.95% and 31.27% after the addition of 0.1 M and 0.2 M NaCl,
247 respectively (Figure 1B and 1D and Table S2). When NaCl concentrations greater than 0.2 M
248 were added, lipid content decreased significantly as salinity increased (Figure 1D and Table S2).

249   Carbohydrate content gradually increased early in cultivation (days 1–12) but decreased
250 rapidly as total lipid content increased after day 12. At day 24, carbohydrate contents were 0.74-,
251 0.88-, 0.62-, 0.53-, and 0.38-fold that of the control in the 0.1, 0.2, 0.4, 0.6, and 0.8 M NaCl
252 addition treatments, respectively (Figure 1C and Table S2). By contrast, the lipid contents of the
253 same treatments were 1.37-, 1.43-, 1.20-, 1.15-, and 1.13-fold that of the control (Figure 1D and
254 Table S2). At the same time, the stability of the specific growth rate of cells under low salt stress
255 (0.1 and 0.2 M NaCl addition) was higher than that under medium and high salt stress (0.4–0.8
256 M NaCl addition), resulting in low lipid productivity under high salt stress (Figure 1E and 1F
257 and Table S2). This is consistent with the change in lipid content.

258   The biomass of *Chlorella* sp. TLD6B was significantly correlated with its physiological
259 parameters on day 18 of salt stress. Cell density (OD_{680}) and carbohydrate content were
260 significantly correlated with biomass on day 18, but the correlation between biomass and total
261 lipid content was highest ($r = 0.79$) (Table 1). Therefore, *Chlorella* cells under low salt stress
262 (0.1 M NaCl addition) and high salt stress (0.8 M NaCl addition) on day 18 were selected for
263 transcriptome sequencing to further study the mechanisms of lipid accumulation under salt
264 stress.

265 **RNA-sequencing, *de novo* transcriptome assembly, and functional annotation**

266 RNA-seq was performed on the mRNA extracted from the two NaCl treatments and the control,
267 generating 963,078,184 raw reads. A total of 947,225,244 clean reads were obtained after
268 filtering on base quality score and read length. The GC percentage of the clean reads was nearly
269 66.0%, and the Q20 was greater than 96% (Table S3). Trinity was used to create a *de novo*
270 transcriptome assembly from the high-quality clean reads, producing 219,577 transcripts with an

271   average length of 1,394 bp. 155,503 non-redundant unigenes were assembled; their length
272   ranged from 200 to 23,825 bp with an average length of 1,842 bp (Tables S4 and S5).
273   All assembled unigenes were functionally annotated by searching against multiple public
274   databases. Of the 155,503 unigenes, 111,238, 60,439, 84,173, 105,026, 109,098, and 51,484
275   were successfully annotated in the NR, NT, SwissProt, PFAM, GO, and KOG databases,
276   respectively. Unigenes were also functionally annotated by searching against the KEGG
277   database. A total of 47,032 (30.24%) unigenes had an annotated function in the KEGG database,
278   and 131,623 (84.64%) unigenes were successfully annotated in at least one database (Table 2).

279   **DEGs in response to salt stress**

280   There were a total of 16,402 DEGs across the low salinity (0.1 M NaCl addition, Nacl1) and high
281   salinity (0.8 M NaCl addition, Nacl2) treatments, based on thresholds of $P < 0.05$ and $|\log2FC| \geq$
282   1 (Figure 2A and Table S6). Of these, 1,326 were up-regulated and 2,304 were down-regulated
283   under low salinity, and 9,776 were up-regulated and 5,798 were down-regulated under high
284   salinity. Eight hundred twenty-eight unigenes were differentially expressed only under low
285   salinity, 12,772 were differentially expressed only under high salinity, and 2,802 were
286   differentially expressed under both conditions (Figure 2B and Table S6). Of the 16,402 total
287   DEGs, 82.9% were differentially expressed under only the low or the high salinity treatment.

288   **qRT–PCR verification of RNA-seq data**

289   Nine DEGs in Nacl1 vs. CK18 (the 0.1 M NaCl treatment compared to the control on day 18)
290   and Nacl2 vs. CK18 (the 0.8 M NaCl treatment compared to the control on day 18) were selected
291   for qRT–PCR verification. These unigenes were mainly involved in fatty acid synthesis, TAG
292   synthesis, the glycolysis/gluconeogenesis pathway, the pentose phosphate pathway, and energy
293   metabolism of the mitochondrial respiratory chain. Seven were up-regulated and two were down-
294   regulated. The qRT–PCR primers listed in Table S7 were used to verify the RNA-seq data (Table
295   S7), and the results are shown in Fig. 3A and Table S7. The expression patterns of nine unigenes
296   were similar in the qRT–PCR and RNA-seq data, although there was some deviation in fold
297   change values between the two methods. The qRT–PCR results were highly correlated with the
298   RNA-seq results ($r = 0.890$, $r^2 = 0.791$), indicating that the RNA-seq data were generally
299   accurate and reliable (Figure 3B).

300   **GO and KEGG pathway enrichment analysis of the DEGs**

301   To further explore their functions, the DEGs from the two salt treatments were annotated with
302   GO terms and KEGG pathways for functional and pathway enrichment analyses (Table S6).
303   Among the top 30 most highly enriched GO terms in the 828 specific DEGs from the low
304   salinity treatment, one molecular function (MF) GO term was significantly enriched (corrected P
305   value < 0.05): transferase activity, transferring one-carbon groups (GO:0016741). Among the top
306   30 most highly enriched GO terms in the 2,802 common DEGs, 10 biological process (BP) terms
307   and 20 MF terms were significantly enriched (corrected P value < 0.05). In the BP category, the
308   three most significantly enriched GO terms were G protein-coupled receptor signaling pathway

309 (GO:0007186), defense response to other organism (GO:0098542), and response to external
310 biotic stimulus (GO:0043207). The three most significantly enriched MF GO terms were
311 peptidase activity (GO:0008233), peptidase activity, acting on L-amino acid peptides
312 (GO:0070011), and endopeptidase activity (GO:0004175). The most strongly and significantly
313 enriched BP GO term in the 12,772 specific DEGs from the high salinity treatment was
314 transcription initiation from RNA polymerase II promoter (GO:0006367). The three most
315 significantly enriched cellular component (CC) GO terms were RNA polymerase II transcription
316 factor complex (GO:0090575), nuclear transcription factor complex (GO:0044798), and
317 transcription factor TFIIA complex (GO:0005672). The most significantly enriched MF GO term
318 was secondary active transmembrane transporter activity (GO:0015291) (Figure 4 and Table S8).
319 There were no significantly enriched KEGG pathways in the low salinity-specific DEGs. Among
320 the top 20 KEGG pathways enriched in the common DEGs, seven were significantly enriched
321 (corrected P value < 0.05): plant hormone signal transduction (ko04075), arginine and proline
322 metabolism (ko00330), glutathione metabolism (ko00480), betalain biosynthesis (ko00965),
323 sulfur metabolism (ko00920), cysteine and methionine metabolism (ko00270), and nitrogen
324 metabolism (ko00910). The 12,772 high salinity-specific DEGs were significantly enriched in
325 mismatch repair (ko03430), DNA replication (ko03030), nucleotide excision repair (ko03420),
326 proteasome (ko03050), photosynthesis (ko00195), porphyrin and chlorophyll metabolism
327 (ko00860), and galactose metabolism (ko00052) (Figure 5 and Table S9). Consistent with the
328 KEGG analysis, GO enrichment analysis showed that common DEGs under low and high
329 salinity were involved primarily in stress response, defense response, and membrane structure.

330 **Transcriptional expression of unigenes involved in fatty acid and TAG biosynthesis**
331 **pathways**

332 *Fatty acid biosynthesis*

333 Acetyl-CoA, the precursor for fatty acid synthesis in the cytosol, derives from pyruvate (PYR)
334 produced in glycolysis by pyruvate kinase (PK). Genes encoding two rate-limiting enzymes in
335 glycolysis, hexokinase (HXK) and PK, were up-regulated under both the high and low salinity
336 treatments, and 6-phosphofructokinase (PFK) was up-regulated under the high salinity treatment
337 (Figure 6 and Table S10). These changes would have promoted the accumulation of acetyl-CoA
338 and energy.
339   The expression of key genes of the *de novo* fatty acid synthesis pathway also changed in
340 response to salinity treatment. For example, the acetyl CoA carboxylase (ACCase) genes *BC* and
341 *BCCP* were up-regulated on day 18 under both salinity treatments. The *α-CT* gene (Cluster-
342 31803.29741) was up-regulated 2.7-fold under high salinity (Figure 7A and Table S11), and the
343 malonyl-CoA:ACP transacylase (*MCTA*) gene (Cluster-31803.71595) was also up-regulated only
344 under high salinity (Figure 7B and Table S11). Two 3-oxoacyl-[acyl carrier protein] synthase II
345 (*KAS II*) genes (Cluster-31803.17167 and Cluster-31803.96146) were up-regulated under both
346 salinity treatments, but these differences were not significant (Figure 7C and Table S11). One ω-
347 3 fatty acid desaturase (*FAD*) gene (Cluster-31803.83020) was down-regulated 4.5-fold under

348 high salinity, and the other *FAD* gene (Cluster-31803.96909) was up-regulated 1.5-fold under
349 low salinity (Figure 7D and Table S11). A stearoyl ACP desaturase (*SAD*) gene (Cluster-
350 31803.15683) was down-regulated under low salinity, whereas three *SAD* genes were up-
351 regulated under high salinity (Cluster-31803.73844, Cluster-31803.73842, and Cluster-
352 31803.73850) (Figure 7E and Table S11).

353 ***TAG biosynthesis***

354 Four NAD-3-phosphate glycerol dehydrogenase (*GPD*) genes and one glycerol kinase (*GK*) gene
355 were significantly up-regulated under high salinity. A gene encoding the glycolysis enzyme
356 triose-phosphate isomerase (TPI) was up-regulated under both salinity treatments, which may
357 have resulted in the accumulation of DHAP (Figures 6, 8A, 8B, and 8C and Table S12) and
358 promoted the synthesis of TAG. One *DGAT1* gene and seven *DGAT2* genes were identified in
359 our transcriptome data. All but two were up-regulated (Cluster-31803.65991 and Cluster-
360 31803.86613) (Figures 6, 8D and Table S12).

361 **Expression of key unigenes related to lipid synthesis pathways**

362 To further explore mechanisms of lipid accumulation in *Chlorella* sp. TLD6B under salt stress,
363 we compared the expression of genes associated with the metabolic pathways of starch-lipid
364 biosynthesis. Under high salinity, a single gene encoding the starch-degrading enzyme α-amylase
365 (*AMY3*, Cluster-31803.62982) was up-regulated 4.6-fold (Figure 6 and Table S10).
366   Furthermore, genes encoding ACL, PDC/PDH, ME, G6PD, and PEPC were primarily up-
367 regulated. All of these genes showed greater expression under high salinity than under low
368 salinity (Figure 6 and Table S10). The upregulation of these genes whose products function in
369 central carbon metabolism may directly or indirectly promote the accumulation of fatty acids.

370 **DISCUSSION**

371 High salinity is generally not conducive to the growth and development of organisms because of
372 Na$^+$ toxicity, excessive ROS accumulation, and difficulties related to osmotic balance and water
373 absorption. The salt tolerance mechanisms of different microalgae may differ. To date, many
374 studies have shown that salt treatment strongly promotes lipid synthesis in microalgae but also
375 inhibits cell growth (*Sharma et al., 2012; Fan et al., 2014; Kato et al., 2017; Li et al., 2018*).
376 According to current research, marine microalgae have higher salt tolerance than other algae
377 such as *Dunaliella salina* (*Takagi et al., 2006; Benmoussa-Dahmen et al., 2016*). By analyzing
378 salt resistance and lipid content, we found that *Chlorella* sp. TLD6B could tolerate high levels of
379 salt stress (0.8 M NaCl addition) that are lethal to many other freshwater algae (*Li et al., 2018*).
380 *Chlorella* sp. TLD6B showed greater lipid accumulation following addition of 0.1 and 0.2 M
381 NaCl, but this effect decreased at higher salt levels. This result indicates that *Chlorella* sp.
382 TLD6B has a mechanism for increasing lipid accumulation under salt stress. By extension, the
383 addition of 0.1 or 0.2 M NaCl can significantly promote *Chlorella* sp. TLD6B lipid accumulation
384 and potentially reduce the production costs of biodiesel.

385   The salinity-induced accumulation of lipids in microalgae begins with a signal transduction
386   cascade initiated by the perception of a salt stress signal. Downstream results include an increase
387   in lipid and unsaturated fatty acid concentrations, the rapid accumulation of solutes that regulate
388   cellular osmotic balance (soluble sugars, amino acids, and betaine), and the induction of the ROS
389   scavenging system (*Ramos et al., 2011*). Here, we found that many key genes involved in
390   glycerol, fatty acid, and lipid metabolism were significantly up-regulated in response to different
391   salinity treatments, suggesting that the salt tolerance of *Chlorella* sp. TLD6B is related to its
392   lipid metabolism. Low levels of NaCl addition up-regulated the expression of genes related to
393   fatty acid synthesis (*BC*, *BCCP*, *KAS II*) and promoted increased biomass and lipid production,
394   indicating that low salinity is essential for the growth of *Chlorella* sp. TLD6B and ultimately
395   promotes its lipid accumulation. Nonetheless, the regulation of lipid accumulation through the
396   manipulation of salinity levels requires further study. Rao et al. (*2007*) reported that increased
397   salt concentration in the growth medium altered the membrane lipid composition of
398   *Botryococcus braunii* LB 572 cells: the proportion of stearic and linoleic acid decreased, and that
399   of oleic acid rose. These results suggested that unsaturated fatty acids play a role in salt
400   tolerance.
401   Previous studies have also shown that SAD is a key enzyme for the synthesis and
402   metabolism of unsaturated fatty acids, directly determining the total amount of unsaturated fatty
403   acids in vegetable oils as well as the ratio of saturated to unsaturated fatty acids (*Kachroo et al.,*
404   *2007*). *FAD* is considered to be a candidate gene for the promotion of high oleic acid levels
405   (*Jung et al., 2000a*). Schwartzbeck et al. (*2001*) used transgenic technology to inhibit FAD2
406   enzyme activity and increase the oleic acid content of corn oil from 25% to 64%. Jung et al.
407   (*2000b*) increased the ratio of oleic acid to linoleic acid in peanuts by inhibiting FAD2 enzyme
408   activity. Here, we also found that high salinity up-regulated *SAD* expression in *Chlorella* sp.
409   TLD6B, whereas low salinity down-regulated *SAD* expression. One *FAD* gene (Cluster-
410   31803.83020) was down-regulated 4.5-fold under high salinity, whereas another (Cluster-
411   31803.96909) was up-regulated 1.5-fold under low salinity (Figure 7D). This indicates that *SAD*
412   and *FAD* may be involved in the regulation of fatty acid components in *Chlorella* sp. TLD6B.
413   Low salinity may promote fatty acid synthesis, whereas high salinity may enhance unsaturated
414   fatty acid synthesis, thereby reducing damage to cell membranes during salt stress (*Kan et al.,*
415   *2012*). The lipid content of *Chlorella* sp. TLD6B increases under high salinity, and it is unknown
416   whether the unsaturated fatty acid content also increases. Although we did not measure fatty acid
417   composition, the transcriptome data indicated that *SAD* genes were up-regulated and an *FAD*
418   gene was down-regulated under high salinity. This result suggests that the unsaturated fatty acid
419   content may increase under high salt stress to reduce cell membrane damage.
420   Our results revealed that the pathway of lipid synthesis in *Chlorella* sp. TLD6B is finely
421   regulated in response to different salinity conditions. First, upregulation of the key glycolysis
422   genes *HXK* and *PK*, which implies enhancement of pentose phosphate metabolism, was likely to
423   promote rapid acetyl-CoA accumulation and a stable intracellular energy supply. Therefore, high
424   glycolysis rates may be one reason for the high lipid accumulation observed in *Chlorella* sp.

425   TLD6B in response to NaCl addition. Second, ACCase catalyzes the formation of malonyl-CoA
426   from acetyl-CoA and is the primary rate-limiting enzyme for *de novo* fatty acid synthesis.
427   Upregulation of the corresponding gene may increase the rate of fatty acid synthesis (*Roesler et*
428   *al., 1997; Zalutskaya et al., 2015*). We found that key genes of fatty acid synthesis, *ACCase* (*BC*
429   and *BCCP*) and *KAS II*, were up-regulated after the addition of NaCl (Figure 7A, 7C), which
430   may also have enhanced fatty acid synthesis. Moreover, *ACL*, *PDC/PDH*, and *ME* in the PDH
431   bypass were up-regulated, which may have accelerated the accumulation of precursor substrates
432   and energy for fatty acid biosynthesis (*Tan & Lee, 2016*). The presence and high expression of
433   these genes suggest that *Chlorella* sp. TLD6B uses a specific approach to ensure the rapid
434   biosynthesis of fatty acids and TAG. Finally, the fatty acyl-CoA produced by *de novo* synthesis
435   is esterified to produce TAG. The synthesis of TAG requires not only fatty acids but also
436   glycerol 3-phosphate (G3P) (*Ohlrogge & Browse, 1995*). G3P is synthesized from glycerol by
437   glycerol kinase (GK) or from DHAP by NAD-3-phosphate glycerol dehydrogenase (GPD) (*Yao*
438   *et al., 2014; Huang et al., 2016*) (Figures 6, 8B and 8C). In addition, research has shown that the
439   overexpression of *GPDH* in microalgae promotes the conversion of DHAP to G3P (*Yao et al.,*
440   *2014*) and that overexpression of fatty acid synthesis genes such as *ACCase* increases lipid
441   accumulation (*Courchesne et al., 2009*). Both of these pathways compete for precursor
442   substrates, and the flux of carbon out of glycolysis towards glycerol formation can cause cell
443   growth to be inhibited. In our transcriptome data, four *GPD* genes and one *GK* gene were
444   significantly up-regulated under high salt stress, and two *TPI* genes were up-regulated under both
445   low and high salinity; these changes are beneficial to TAG synthesis but may inhibit cell growth.
446   Therefore, salt stress only moderately increases the lipid concentration. This may explain why, in
447   our study, carbohydrate levels gradually declined under salt stress while lipid accumulation
448   increased. Moreover, the total lipid concentration under high salinity decreased to that of the
449   control and was lower than the total lipid concentration under low salinity (Figure 1D).
450   Therefore, we suggest that salt stress alters the carbon flow between starch biosynthesis and lipid
451   biosynthesis in *Chlorella* sp. TLD6B.
452   In addition, recent transcriptome studies have shown that microalgal lipid synthesis may be
453   influenced by the conversion between starch and lipid synthesis (*Shang et al., 2016; Ho et al.,*
454   *2017*). Here, only one *AMY3* gene (Cluster-31803.62982) was up-regulated 4.6-fold under high
455   salinity. Lipid synthesis in *Chlorella* sp. TLD6B may therefore not be closely related to the
456   conversion between starch and lipid biosynthesis. Its lipid accumulation may be controlled
457   primarily by glycolysis and the synthesis of fatty acids and TAG.

458   **CONCLUSION**

459   We performed physiological measurements and genome-wide transcriptome profiling of
460   *Chlorella* sp. TLD6B under different levels of salt stress. *Chlorella* sp. TLD6B was able to
461   tolerate high salt stress (0.8 M NaCl addition). Lipid concentration first increased and then
462   decreased with increasing levels of salt stress, reaching a maximum under the addition of 0.2 M
463   NaCl. Comparative transcriptomic analysis revealed that salt stress enhanced the expression of
464   genes related to sugar metabolism and fatty acid biosynthesis (the *ACCases BC* and *BCCP*, *KAS*

465 *II*, and *GPDHs* involved in TAG synthesis), thereby promoting lipid accumulation under the
466 addition of 0.2 M NaCl. However, high salt stress also inhibited cell growth. Expression of three
467 *SADs*, whose encoded products function in unsaturated fatty acid biosynthesis, was up-regulated
468 under high salinity (0.8 M NaCl addition). This research clarifies the relationship between salt
469 tolerance and lipid accumulation, promoting the development and utilization of *Chlorella* sp.
470 TLD6B for biofuel production.

471

Funding

473 This study was supported by the National Natural Science Foundation of China (31460276) and
474 the Shihezi University independently funded Project (ZZZC201840B). The funders had no role
475 in study design, data collection and analysis, decision to publish, or preparation of the
476 manuscript.

Grant Disclosures

478 The following grant information was disclosed by the authors:
479 National Natural Science Foundation of China: 31460276.
480 Shihezi University independently funded Project: ZZZC201840B.

Competing Interests

482 The authors declare there are no competing interests.

Author Contributions

484 • Hong Li performed the experiments, analyzed the data, prepared the figures and/or tables, and
485 wrote and reviewed drafts of the paper.
486 • Jun Tan performed experiments and prepared figures and/or tables.
487 • Yun Mu performed experiments, prepared figures and/or tables, and analyzed the data.
488 • Jianfeng Gao conceived and designed the experiment, reviewed drafts of the paper, and
489 approved the final draft.

Data Availability

491 The following information was supplied regarding data availability: *Chlorella* sp. TLD6B
492 transcriptome sequence data are available at NCBI GEO under accession numbers: GSE162916.
493 Raw data are available in the Supplemental Files.

Acknowledgments

495 The authors would like to thank TopEdit (www.topeditsci.com) for linguistic assistance during
496 preparation of this manuscript.

Supplemental Information

498 Supplemental information for this article can be found online at ***.

499

REFERENCES

501 **Anders S, Huber W. 2010.** Differential expression analysis for sequence count data. *Genome Biology*
502 **11(10)**:R106 DOI 10.1186/gb-2010-11-10-r106.

503 **Ashley J, Rushforth, SR. 1984.** Growth of soil algae on top soil and processed oil shale from the Uintah
504 Basin, Utah, U.S.A. *Reclamation and Revegetation Research* 3:49-63 DOI 10.1007/BF01407604.

505 **BenMoussa-Dahmen I, Chtourou H, Rezgui F, Sayadi S, Dhouib A. 2016.** Salinity stress increases lipid,
506 secondary metabolites and enzyme activity in *Amphora subtropica* and *Dunaliella* sp. for biodiesel
507 production. *Bioresource Technology* **218**:816-825 DOI 10.1016/j.biortech.2016.07.022.

508 **Courchesne NMD, Parisien A, Wang B, Lan CQ. 2009.** Enhancement of lipid production using
509 biochemical, genetic and transcription factor engineering approaches. *Journal of Biotechnology* **141(1-**
510 **2)**:31-41 DOI 10.1016/j.jbiotec.2009.02.018.

511 **Davidson NM, Oshlack A. 2014.** Corset: enabling differential gene expression analysis for de novo
512 assembled transcriptomes. *Genome Biology* **15(7)**:410 DOI 10.1186/s13059-014-0410-6.

513 **Dubois M, Gilles HA, Hamilton JK, Rebers PA. 1956.** Colorimetric method for determination of sugars and
514 related substances. *Analytical Chemistry* **28(3):**22-25 DOI 10.1021/ac60111a017.

515 **Fan JH, Cui YB, Wan MX, Wang WL, Li YG. 2014.** Lipid accumulation and biosynthesis genes response
516 of the oleaginous *Chlorella pyrenoidosa* under three nutrition stressors. *Biotechnology for Biofuels* **7**:17
517 DOI 10.1186/1754-6834-7-17.

518 **Gao CF, Wang Y, Shen Y, Yan D, He X, Dai JB. Wu QY. 2014.** Oil accumulation mechanisms of the
519 oleaginous microalga *chlorella prototothecoides* revealed through its genome, transcriptomes, and
520 proteomes. *BMC Genomics* **15**:582 DOI 10.1186/1471-2164-15-582.

521 **Garcia-Pichel F, Lopez-Cortes A, Nubel U. 2001.** Phylogenetic and morphological diversity of
522 cyanobacteria in soil desert crusts from the Colorado Plateau. *Applied and Environmental*
523 *Microbiology* **67**:1902-1910 DOI 10.1128/AEM.67.4.1902-1910.2001.

524 **Gong CX, Li FF, Gou YF, Wang D, Gao JF. 2013.** Comparison of different culture methods for a desert
525 *chlorella*. *Renewable Energy Resources* **31(11)**:106-115.

526 **Grabherr MG, Haas BJ, Yassour M, Levin JZ, Thompson DA, Amit I, Adiconis X, Fan**
527 **L, Raychowdhury R, Zeng Q, Chen Z, Mauceli E, Hacohen N, Gnirke A, Rhind N, Palma FD,**
528 **Birren BW, Nusbaum C, Lindblad-Toh K, Friedman N, Regev A. 2011.** Full-length transcriptome
529 assembly from RNA-Seq data without a reference genome. *Nature Biotechnology* **29**:644-652 DOI
530 10.1038/nbt.1883.

531 **Götz S, García-Gómez JM, Terol J, Williams TD, Nagaraj SH, Nueda MJ, Robles M, Robles M, Dopazo**
532 **J, Conesa A. 2008.** High-throughput functional annotation and data mining with the Blast2GO suite.
533 *Nucleic Acids Research* **36**:3420-3435 DOI 10.1093/nar/gkn176.

534 **Halim R, Danquah MK, Webley PA. 2012.** Extraction of oil from microalgae for biodiesel production: A
535 review. *Biotechnology Advances* **30**:709-732 DOI 10.1016/j.biotechadv.2012.01.001.

536 **Ho SH, Nakanish A, Ye X, Chang JS, Hara K, Hasunuma T, Kondo A. 2014.** Optimizing biodiesel
537 production in marine *Chlamydomonas* sp. JSC4 through metabolic profiling and an innovative salinity-
538 gradient strategy. *Biotechnology for Biofuels* **7**:97 DOI 10.1186/1754-6834-7-97.

539 **Ho SH, Nakanishi A, Kato Y, Yamasaki H, Chang JS, Misawa N, Hirose Y, Minagawa J, Hasunuma T,**
540 **Kondo A. 2017.** Dynamic metabolic profiling together with transcription analysis reveals salinity-
541 induced starch-to-lipid biosynthesis in alga *chlamydomonas* sp. JSC4. *Scientific Reports* **7**:45471 DOI
542 10.1038/srep45471.

543 **Huang WP, Ye JR, Zhang JJ, Lin Y, He MX, Huang JC. 2016.** Transcriptome analysis of *chlorella*

544   *zofingiensis* to identify genes and their expressions involved in astaxanthin and triacylglycerol
545   biosynthesis. *Algal Research* **17**:236-243 DOI 10.1016/j.algal.2016.05.015.

546 **Jung S, Powell G, Moore K, Abbott A. 2000a.** The high oleate trait in the cultivated peanut (Arachis
547   hypogaea L.). II. Molecular basis and genetics of the trait. *Molecular Genetics and Genomics* **263(5)**:806-
548   811 DOI 10.1007/s004380000243.

549 **Jung S, Swift D, Sengoku E, Patel M, Teulé F, Powell G, Moore K, Abbott A. 2000b.** The high oleate trait
550   in the cultivated peanut (Arachis hypogaea L.). I. Isolation and characterization of two genes encoding
551   microsomal oleoyl-PC desaturases. *Molecular & General Genetics Mgg* **263(5)**:796-805 DOI
552   10.1007/s004380000244.

553 **Kachroo A, Shanklin J, Whittle E, Lapchyk L, Hildebrand D, Kachroo P. 2007.** The Arabidopsis stearoyl-
554   acyl carrier protein-desaturase family and the contribution of leaf isoforms to oleic acid synthesis. *Plant*
555   *Molecular Biology* **63(2)**:257-271 DOI 10.1007/s11103-006-9086-y.

556 **Kan GF, Shi CJ, Wang XF, Xie QJ, Wang M, Wang XL, Miao JL. 2012.** Acclimatory responses to high-
557   salt stress in *Chlamydomonas* (Chlorophyta, Chlorophyceae) from Antarctica. *Acta Oceanologica Sinica*
558   **31(01)**:116-124 DOI CNKI:SUN:SEAE.0.2012-01-015.

559 **Kato Y, Ho SH, Vavricka CJ, Chang JS, Hasunuma T, Kondo A. 2017.** Evolutionary engineering of salt-
560   resistant, *chlamydomona*ssp. strains reveals salinity stress-activated starch-to-lipid biosynthesis
561   switching. *Bioresource Technology* **245**:1484-1490 DOI 10.1016/j.biortech.2017.06.035.

562 **Langmead B, Salzberg SL. 2012.** Fast gapped-read alignment with Bowtie 2. *Nat Methods* **9(4)**:357-9 DOI
563   10.1038/nmeth.1923.

564 **Lewis LA, Flechtner VR. 2002.** Green algae (Chlorophyta) of Desert microbiotic crusts: Diversity of North
565   American Taxa. *Taxon* **51(3)**: 443-451 DOI 10.2307/1554857.

566 **Li B, Dewey CN. 2011.** RSEM: accurate transcript quantification from RNA-Seq data with or without a
567   reference genome. *BMC Bioinformatics* **12**:323 DOI 10.1186/1471-2105-12-323.

568 **Li FF, Gong CX, Zuo XX, Chen F, Gao JF. 2012.** Crude lipid content and fatty acid composition of six
569   strains of green microalgae in Gurbantunggut desert. *China Oils And Fats* **37(12)**:74-77
570   DOI 10.3969/j.issn.1003-7969.2012.12.019.

571 **Li L, Zhang G, Wang Q. 2016.** De novo transcriptomic analysis of *Chlorella sorokiniana* reveals differential
572   genes expression in photosynthetic carbon fixation and lipid production. *BMC Microbiology* **16**:223 DOI
573   10.1186/s12866-016-0839-8.

574 **Li PL, Miao XL, Li RX, Zhong JJ. 2011.** In situ biodiesel production from fast-growing and high oil content
575   *Chlorella pyrenoidosa* in rice straw hydrolysate. *Journal of Biomedicine & Biotechnology* **7**:141207 DOI
576   10.1155/2011/141207.

577 **Li XY, Yuan YZ, Cheng DJ, Gao J, Kong LZ, Zhao QY, Wei W, Sun YH. 2018.** Exploring stress tolerance
578   mechanism of evolved freshwater strain *Chlorella* sp. S30 under 30 g/L salt. *Bioresource*
579   *Technology* **250**:495-504 DOI 10.1016/j.biortech.2017.11.072.

580 **Liang YN, Sarkany N, Cui Y. 2009.** Biomass and lipid productivities of *Chlorella vulgaris* under autotrophic,
581   heterotrophic and mixotrophic growth conditions. *Biotechnology Letters* **31(7)**:1043-1049 DOI
582   10.1007/s10529-009-9975-7.

583 **Liu J, Huang JC, Sun Z, Zhong YJ, Jiang Y, Chen F. 2011.** Differential lipid and fatty acid profiles of
584   photoautotrophic and heterotrophic *Chlorella zofingiensis*: Assessment of algal oils for biodiesel
585   production. *Bioresource Technology* **102(1)**:106-110 DOI 10.1016/j.biortech.2010.06.017.

586 **Livak KJ, Schmittgen TD. 2001.** Analysis of relative gene expression data using real-time quantitative PCR
587   and the 2(-Delta Delta C(T)) Method. *Methods* **25(4)**:402-408 DOI 10.1006/meth.2001.1262.

588 **Mao XZ, Cai T, Olyarchuk JG, Wei LP. 2005.** Automated genome annotation and pathway identification
589   using the KEGG Orthology (KO) as a controlled vocabulary. *Bioinformatics* **21(19)**:3787–3793 DOI
590   10.2307/1592215.
591 **Markou G, Nerantzis E. 2013.** Microalgae for high-value compounds and biofuels production: A review with
592   focus on cultivation under stress conditions. *Biotechnology Advances* **31(8)**:1532-1542 DOI
593   10.1016/j.biotechadv.2013.07.011.
594 **Mishra SK, Suh WI, Farooq W, Moon M, Shrivastav A, Park MS,Yang JW. 2014.** Rapid quantification of
595   microalgal lipids in aqueous medium by a simple colorimetric method. *Bioresource Technology* **155**:330-
596   333 DOI 10.1016/j.biortech.2013.12.077.
597 **Mu Y, Wang WL, Li H, Yan G, Wang HM, Gao JF. 2016.** Effects of PEG6000 on growth and lipid
598   accumulation of desert *chlorella*. *China Oils and Fats* **41(10)**:58-61.
599 **Nichols HW. 1973.** Growth media – freshwater. In: Stein, J. R. (Ed.), Handbook of Phycological Methods,
600   Culture methods and growth measurements. *Cambridge University Press* **pp**.7-24.
601 **Ohlrogge J, Browse J. 1995.** Lipid biosynthesis. *Plant Cell* **7**:957-970 DOI 10.1105/tpc.7.7.957.
602 **Ramos AA, Polle J, Tran D, Cushman JC, Varela JC. 2011.** The unicellular green alga *Dunaliella salina*
603   Teod. as a model for abiotic stress tolerance: genetic advances and future perspectives. *Algae* **26(1)**:3-20
604   DOI 10.4490/algae.26.1.003.
605 **Rao AR, Dayananda C, Sarada R, Shamala TR, Ravishankar GA. 2007.** Effect of salinity on growth of
606   green alga Botryococcus braunii and its constituents. *Bioresource Technology* **98**:560–564 DOI
607   10.1016/j.biortech.2006.02.007.
608 **Roesler K, Shintani D, Savage L, Boddupalli S, Ohlrogge J. 1997.** Targeting of the Arabidopsis homomeric
609   acetyl-coenzyme A carboxylase to plastids of rapeseeds. *Plant physiology* **113(1)**:75-81
610   DOI 10.1104/pp.113.1.75.
611 **Schenk PM, Thomas-Hall SR, Stephens E, Marx UC, Mussgnug JH, Posten C, Kruse O, Hankamer B.**
612   **2008.** Second Generation Biofuels: High-Efficiency Microalgae for Biodiesel Production. *BioEnergy*
613   *Research* **1**:20-43 DOI 10.1007/s12155-008-9008-8.
614 **Schwartzbeck JL, Jung S, Abbott AG, Mosley E, Lewis S, Pries GL, Powellg L. 2001.** Endoplasmic
615   oleoyl-PC desaturase references the second double bond. *Phytochemistry* **57(5)**:643-652 DOI
616   10.1016/s0031-9422(01)00081-4.
617 **Shang CH, Bi GC, Yuan ZH, Wang ZM, Alam MA, Xie J. 2016.** Discovery of genes for production of
618   biofuels through transcriptome sequencing of *Dunaliella parva*. *Algal Research* **13**:318-326 DOI
619   10.1016/j.algal.2015.12.012.
620 **Sharma KK, Schuhmann H, Schenk PM. 2012.** High lipid induction in Microalgae for Biodiesel Production.
621   *Energies* **5(5)**:1532-1553 DOI 10.3390/en5051532.
622 **Sharma T, Chauhan RS. 2016.** Comparative transcriptomics reveals molecular components associated with
623   differential lipid accumulation between microalgal sp. *Scenedesmus dimorphus* and *Scenedesmus*
624   *quadricauda*. *Algal Research* **19**:109-122 DOI 10.1016/j.algal.2016.07.020.
625 **Srivastava G, Nishchal, Goud VV. 2017.** Salinity induced lipid production in microalgae and cluster analysis
626   (iccb 16-br_047). *Bioresource Technology* **242**:244-252 DOI 10.1016/j.biortech.2017.03.175.
627 **Takagi M, Karseno, Yoshida T. 2006.** Effect of salt concentration on intracellular accumulation of lipids and
628   triacylglyceride in marine microalgae *Dunaliella* cells. *Journal of Bioence and Bioengineering*
629   **101(3)**:223-226 DOI 10.1263 / jbb.101.223.
630 **Tan KW, Lee YK. 2016.** The dilemma for lipid productivity in green microalgae: importance of substrate
631   provision in improving oil yield without sacrificing growth. *Biotechnology for Biofuels* **9**:255
632   DOI 10.1186/s13068-016-0671-2.

633 **Trapnell C, Williams BA, Pertea G, Mortazaviet A, Kwan G, van Baren MJ, Salzberg SL, Wold BJ,**
634   **Pachter L. 2010.** Transcript assembly and quantification by RNA-Seq reveals unannotated transcripts
635   and isoform switching during cell differentiation. *Nature Biotechnology* **28(5)**:511-515 DOI
636   10.1038/nbt.1621.
637 **Yao Y, Lu Y, Peng KT, Huang T, Niu YF, Xie WH, Yang WD, Liu JS, Li HY. 2014.** Glycerol and neutral
638   lipid production in the oleaginous marine diatom *Phaeodactylum tricornutum* promoted by
639   overexpression of glycerol-3-phosphate dehydrogenase. *Biotechnology for Biofuels* **7(1)**:1-9 DOI
640   10.1186/1754-6834-7-110.
641 **Young MD, Wakefield MJ, Smyth GK, Oshlack A. 2010.** Gene ontology analysis for RNA-seq: accounting
642   for selection bias. *Genome Biol* **11(2)**:R14 DOI 10.1186/gb-2010-11-2-r14.
643 **Wan MX, Zhang Z, Wang J, Huang JK, Fan JH, Yu AQ, Wang WL, Li YG. 2015.** Sequential
644   heterotrophy–dilution–photoinduction cultivation of haematococcus pluvialis for efficient production of
645   astaxanthin. *Bioresource Technology* **198**:557-563 DOI 10.1016/j.biortech.2015.09.031.
646 **Wang D, Gong, CX, Gou YF, Zhu L, Zhu JB, Gao JF. 2014.** Phylogenetic analyses on the biological crusts
647   of several algae in the Taklimakan Desert. *Acta Prataculturae Sinica* **23(03)**:97-103.
648 **Wang T, Ge HY, Liu TT, Tian XW, Wang ZJ, Guo MJ, Chu J, Zhuang YP. 2016.** Salt stress induced lipid
649   accumulation in heterotrophic culture cells of *chlorella protothecoides*: Mechanisms based on the multi-
650   level analysis of oxidative response, key enzyme activity and biochemical alteration. *Journal of*
651   *Biotechnology* **228**:18-27 DOI 10.1016/j.jbiotec.2016.04.025.
652 **Zalutskaya Z, Kharatyan N, Forchhammer K, Ermilova E. 2015.** Reduction of PII signaling protein
653   enhances lipid body productionin *Chlamydomonas reinhardtii*. *Plant Science* **240**:1-9 DOI
654   10.1016/j.plantsci.2015.08.019.
655 **Zhao JC, Zhang BC, Zhang YM. 2006.** Study on Chlorophytes of Microbiotic Crusts in the Gurbantonggut
656   Desert, Xinjiang. *Arid Zone Research* **23(2)**:189-194 DOI 10.13866/j.azr.2006.02.001.
657 **Zhang JT, Wang MZ, He Q, Pan HL, Meng L, Wang YH. 2020.** Variation characteristics of nocturnal low-
658   level jet in summer over the hinterland of Taklimakan Desert. *Journal of Desert Research* **40(5)**:89-100.
659 **Zhu JB, Wang D, Gou YF, Wang WL, Gao JF. 2014.** Screening of microalgae rich in lipid in Xinjiang
660   desert. *China Oils and Fats* **39(12)**:68-71 DOI 10.3969/j.issn.1003-7969.2014.12.020.

Figure 1

Figure 1 Effects of different levels of salt stress on the growth, biomass, carbohydrate content, lipid content, specific growth rate, and lipid productivity of *Chlorella* sp. TLD6B.

(A) Growth curves of *Chlorella* sp. TLD6B under different levels of salt stress. (B) Biomass of *Chlorella* sp. TLD6B under different levels of salt stress. (C) Carbohydrate content of *Chlorella* sp. TLD6B under different levels of salt stress. (D) Lipid content of *Chlorella* sp. TLD6B under different levels of salt stress. (E) Specific growth rate of *Chlorella* sp. TLD6B under different levels of salt stress. (F) Lipid productivity of *Chlorella* sp. TLD6B under different levels of salt stress. DW, dry weight. Bars represent SD.
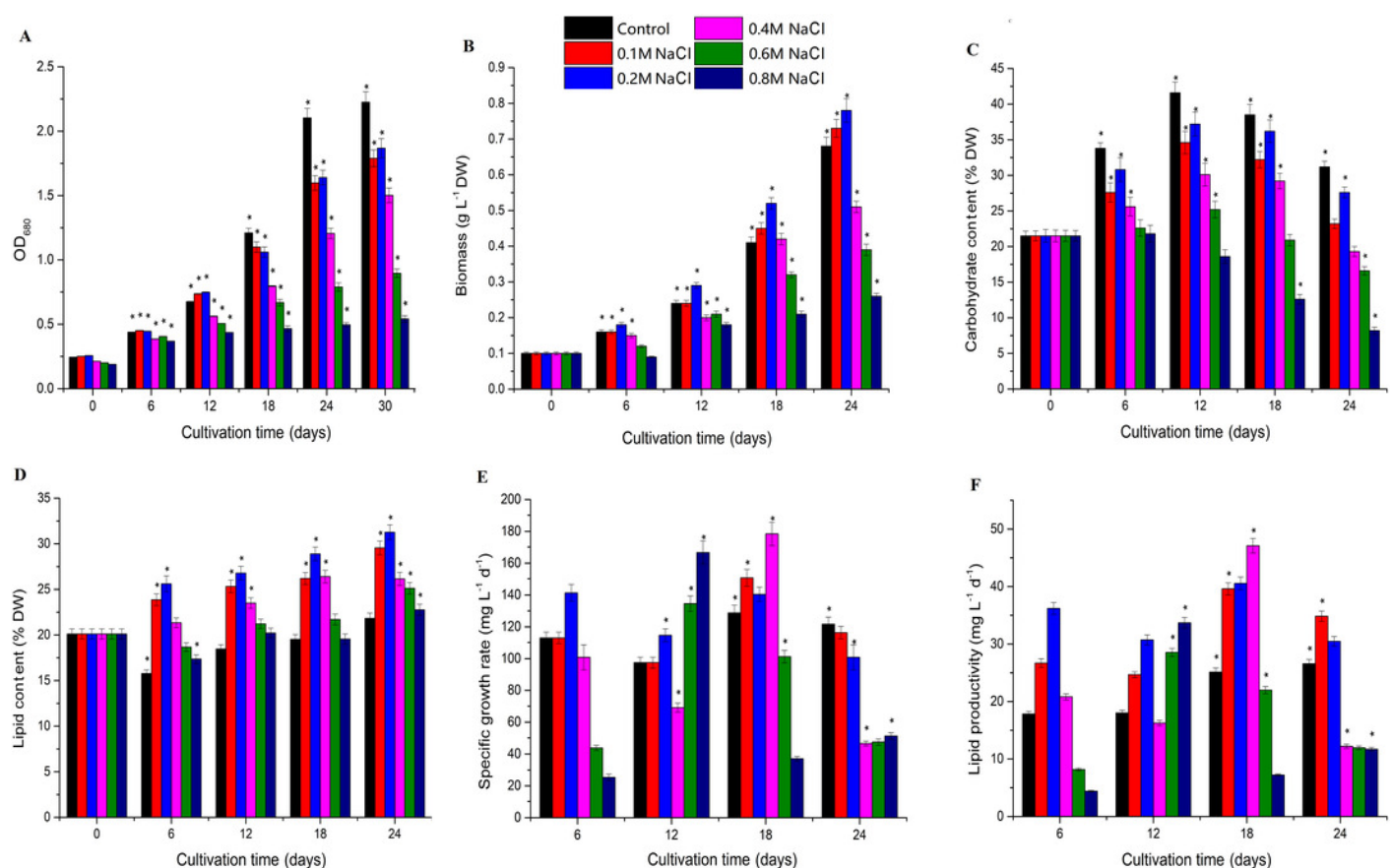
Figure 2

Figure 2 DEGs in the Nacl1 (0.1 M NaCl addition) and Nacl2 (0.8 M NaCl addition) treatments.

(A) A Venn diagram of DEGs in the Nacl1 and Nacl2 treatments. (B) Numbers of up- and downregulated genes in the Nacl1 and Nacl2 treatments.
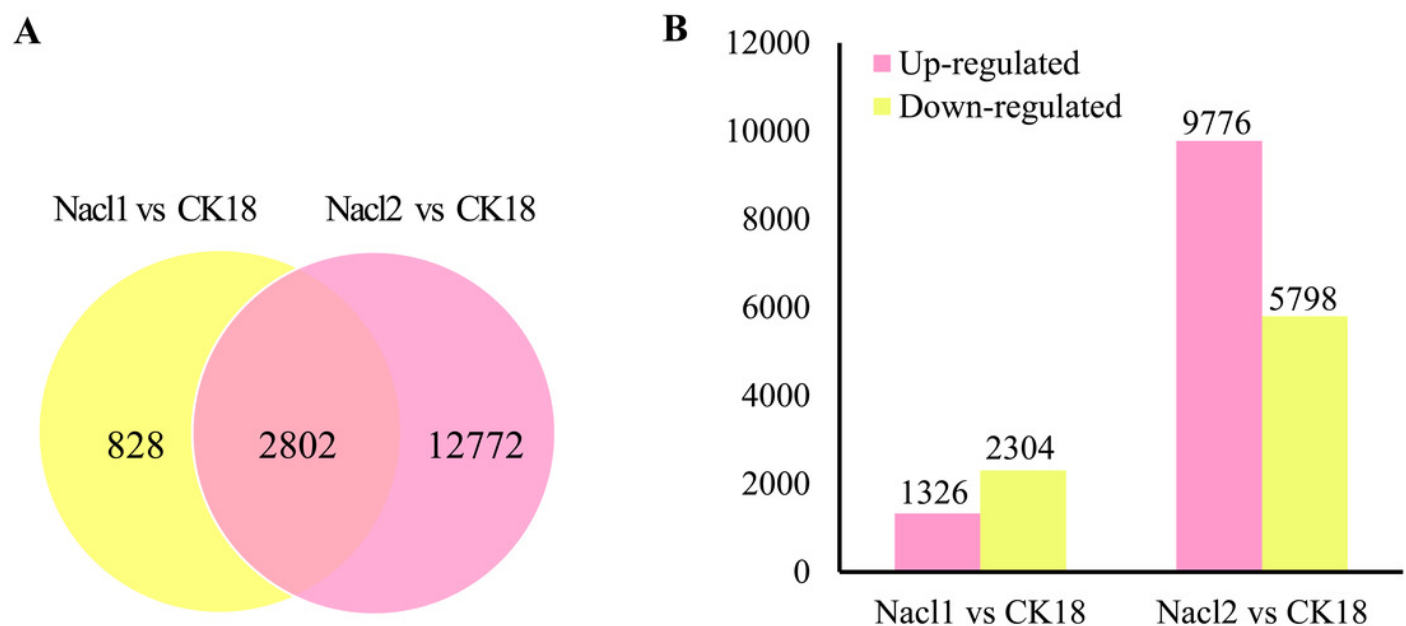
Figure 3

Figure 3 qRT–PCR verification of RNA sequencing results.

(A) Comparison of log2 (fold change) values detected by RNA-seq and qRT–PCR. (B) Correlation between RNA-seq and qRT–PCR values. Log2FC, $\log_2$(fold-change) in gene expression between two groups. BCCP, biotin carboxyl carrier protein of acetyl-CoA carboxylase; KAS II, 3-oxoacyl-[acyl-carrier-protein] synthase II; TPI, triose-phosphate isomerase; PK, pyruvate kinase; PEPC, phosphoenolpyruvate carboxylase; PDC/PDH, pyruvate dehydrogenase; G6PD, glucose-6-phosphate dehydrogenase; 6PGDH, 6-phosphogluconate dehydrogenase; GAPD, glyceraldehyde 3-phosphate dehydrogenase.
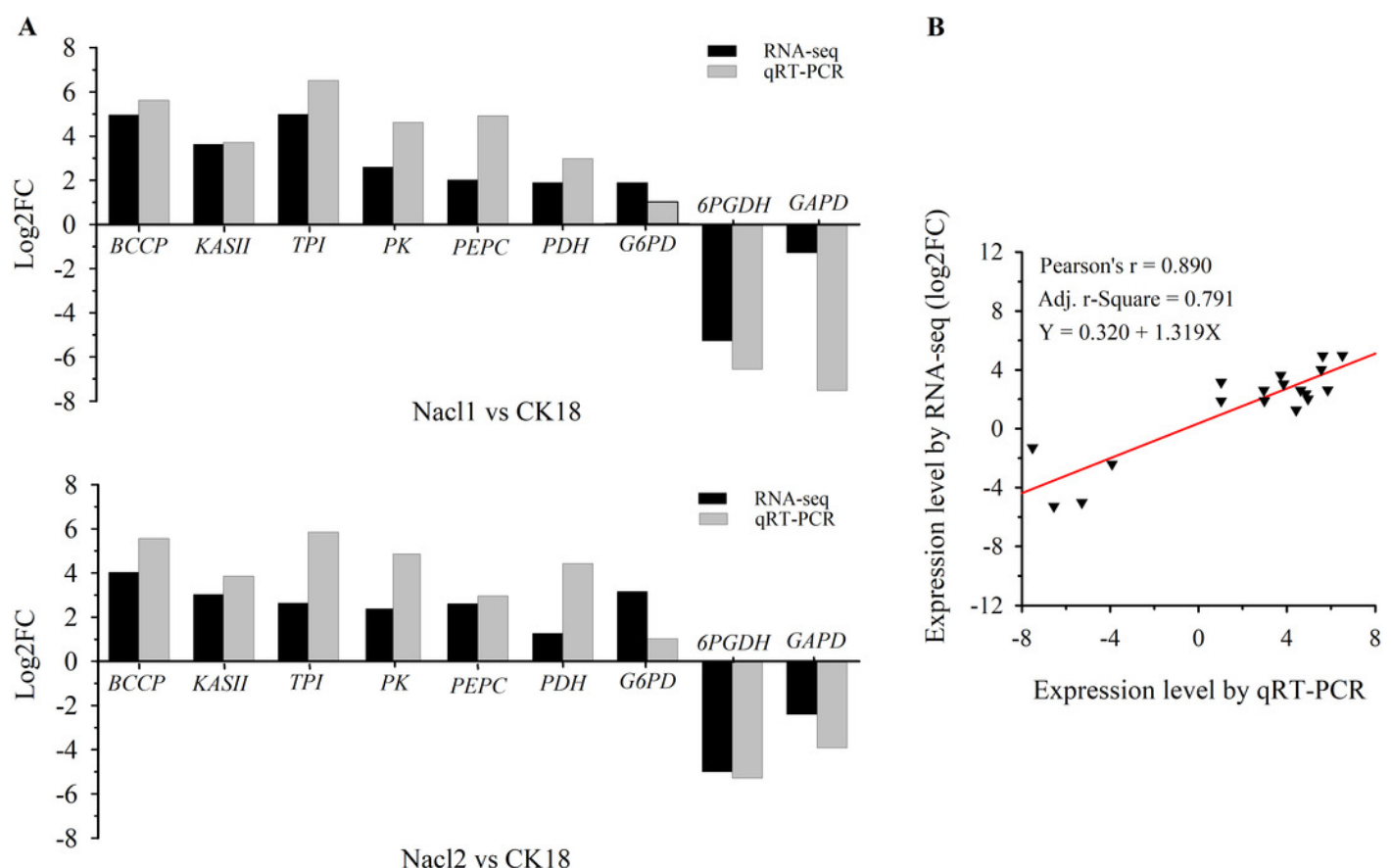
Figure 4

Figure 4 GO enrichment of DEGs under salt stress.

(A) The top 30 most highly enriched GO terms in 828 unigenes specifically differentially expressed under low salinity (0.1 M NaCl addition); (B) The top 30 most highly enriched GO terms in 12,772 unigenes specifically differentially expressed under high salinity (0.8 M NaCl addition); and (C) the top 30 most highly enriched GO terms in 2,802 unigenes differentially expressed under both high and low salinity. The x-axis indicates the number of unigenes in each secondary GO classification. The y-axis indicates the secondary GO classification, and the three colors represent the three major types of GO terms (i.e., BP, CC, and MF). *corrected p-value < 0.05.

A

B

C
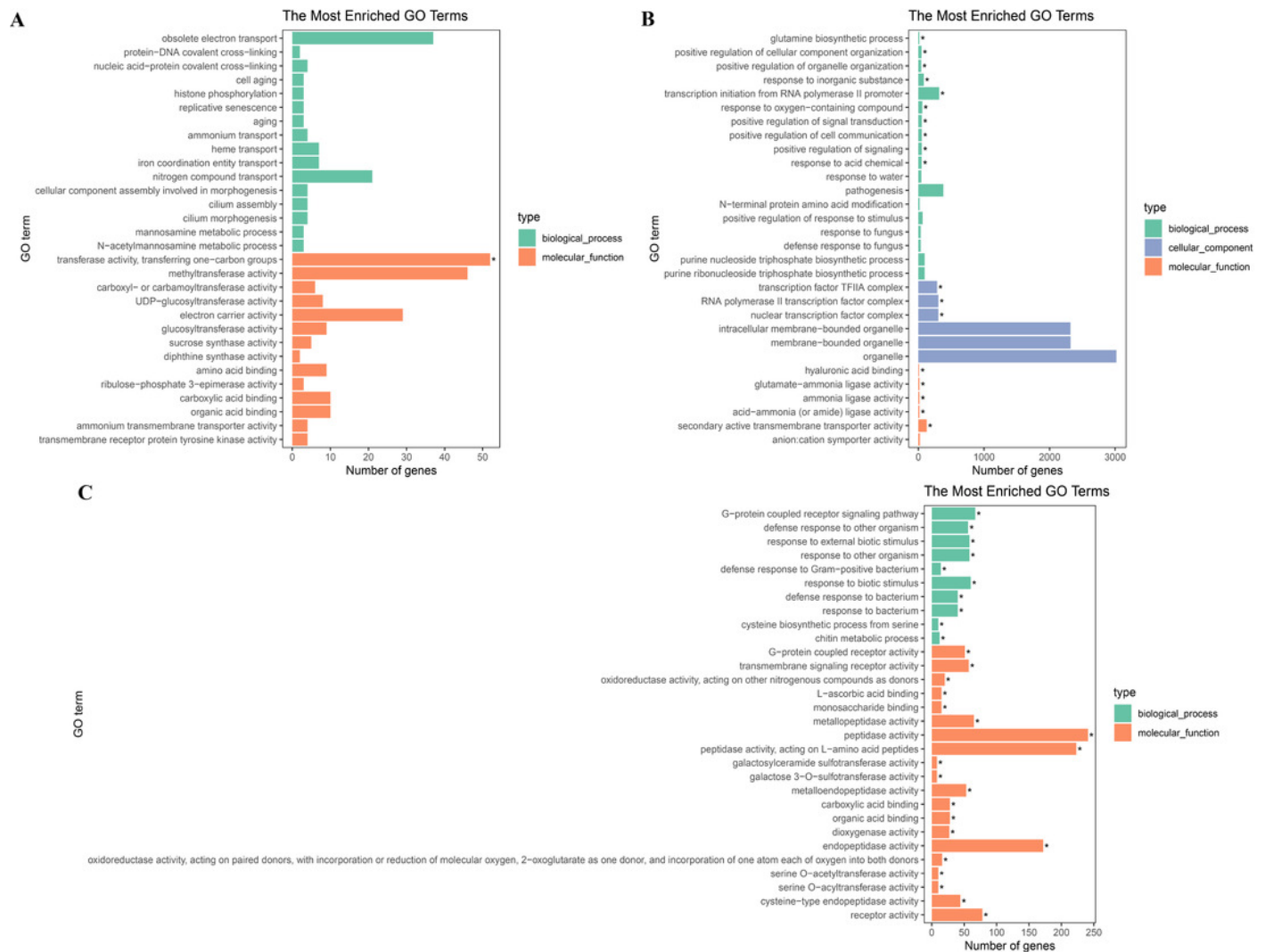
Figure 5

Figure 5 KEGG enrichment of DEGs under salt stress.

(A) The top 20 most highly enriched KEGG pathways in 828 unigenes specifically differentially expressed under low salinity (0.1 M NaCl addition); (B) The top 20 most highly enriched KEGG pathways in 12,772 unigenes specifically differentially expressed under high salinity (0.8 M NaCl addition); and (C) the top 20 most highly enriched KEGG pathways in 2,802 unigenes differentially expressed under both high and low salinity. The names of the pathways and their enrichment factors are shown. The size of the dot indicates the number of genes in a given pathway, and the color of the dot indicates the value of $-\log10$(corrected p value).
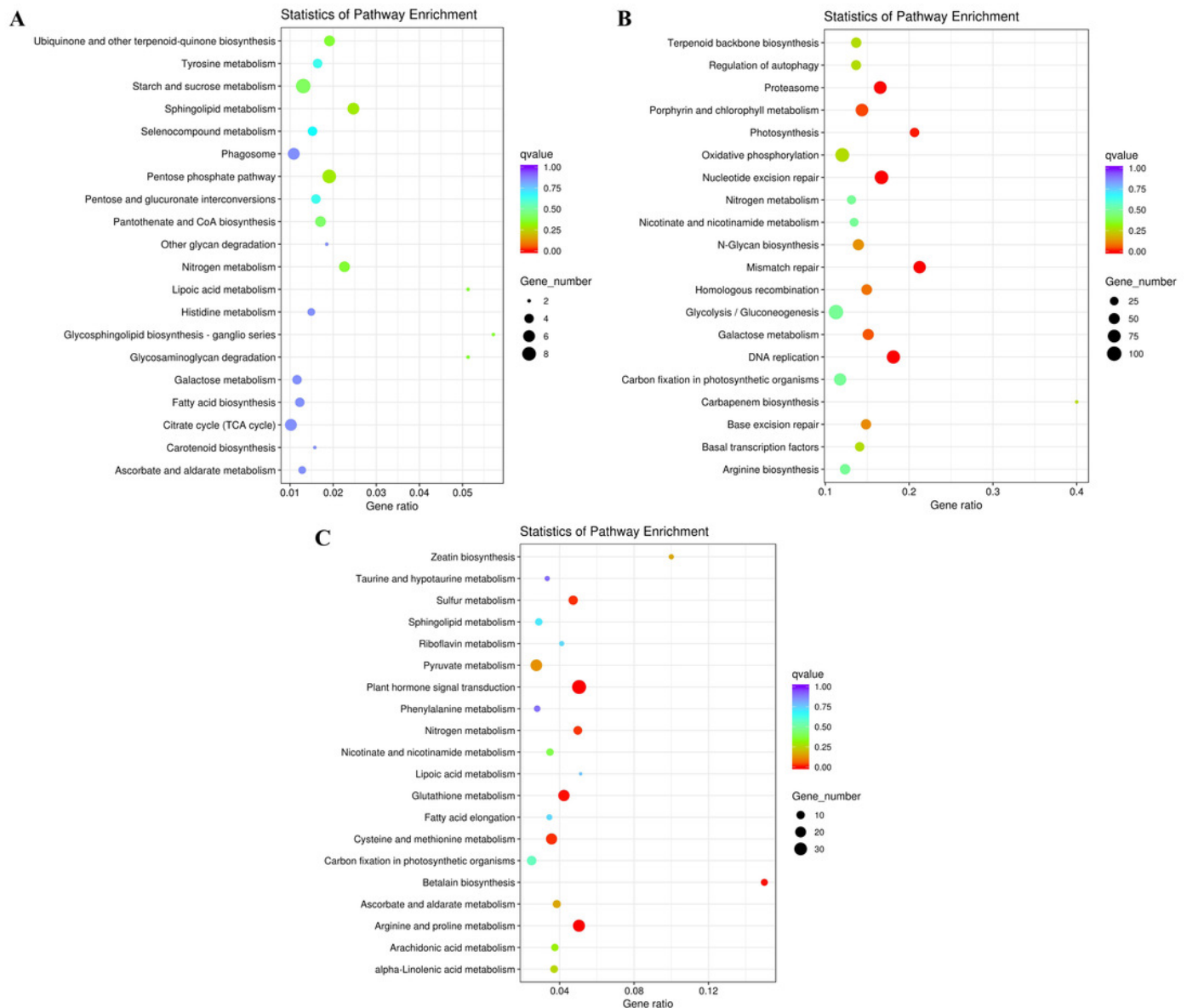
Figure 6

Figure 6 Enzymatic pathways of fatty acid and TAG biosynthesis and the expression of associated genes in response to two levels of salt treatment.

Arrows indicate enzymatic reactions, and red arrows indicate upregulation of the associated genes. Names of key lipid metabolism enzymes whose genes were up-regulated are given in red, names of enzymes whose genes were associated with lipid metabolism are given in blue, and names of enzymes whose genes were not differentially expressed are given in black. "-2" after an enzyme name indicates that its gene was differentially expressed under high salt stress (0.8 M NaCl addition). Enzymes without this designation were differentially expressed under both high and low (0.1 M NaCl addition) salt stress treatments. AMY, α-amylase; HXK, hexokinase; PFK, 6-phosphofructokinase; DHAP, dihydroxyacetone phosphate; GAP, 3-phosphoglyceraldehyde; PYR, pyruvate; G3P, glycerol-3-phosphate; GPD, glycerol-3-phosphate dehydrogenase; GK, glycerol kinase; ACC, acetyl-CoA; ACL, ATP citrate lyase; ME, malic enzyme; LACS, long-chain acyl CoA synthetase; MCAT, malonyl-CoA:acyl-carrier protein transacylase; SAD, stearoyl ACP desaturase; FAD, ω-3 fatty acid desaturase; DGAT, diacylglycerol O-acyltransferase; TAG, triglyceride. Additional abbreviated gene names are defined in Figure 3. Gene expression levels are shown in Figure 7, Figure 8 and Table S10.
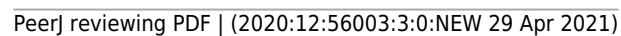
Figure 7

Figure 7 Expression of *Chlorella* sp. TLD6B genes involved in the *de novo* synthesis of fatty acids pathway under low (0.1 M NaCl addition, Nacl1) and high (0.8 M NaCl addition, Nacl2) salt treatments.

(A) Expression of BC/BCCP/α-CT genes; BC, biotin carboxylase of ACCase; α-CT, carboxyltransferase α-subunit; (B) Expression of MCTA gene; (C) Expression of KAS Ⅱ genes; (D) Expression of FAD genes; (E) Expression of SAD genes. Gene IDs such as Cluster-31803.100315 are abbreviated as Cl-3.100315. Additional abbreviated gene names are defined in Figures 3 and 6.

A

RNA-seq (log2FC)

Legend: Nacl1 (black), Nacl2 (red)

Cl-3.98783, Cl-3.100315, Cl-3.101505, Cl-3.78413, Cl-3.29741

Acetyl-CoA

BC/BCCP/a-CT

Malonyl-CoA

MCTA

B

RNA-seq (log2FC)

Legend: Nacl1 (black), Nacl2 (red)

Cl-3.71595

Malonyl-ACP

C16:0-ACP

KAS II

C

RNA-seq (log2FC)

Legend: Nacl1 (black), Nacl2 (red)

Cl-3.17167, Cl-3.96146

C18:0-ACP

D

RNA-seq (log2FC)

Legend: Nacl1 (black), Nacl2 (red)

Cl-3.83020, Cl-3.96909

FAD

SAD

E

RNA-seq (log2FC)

Legend: Nacl1 (black), Nacl2 (red)

Cl-3.73844, Cl-3.73842, Cl-3.73850, Cl-3.15683

SQDG(18:3/16:0)
DGDG(18:3/16:0)
MGDG(18:3/16:3)

C18:1-ACP

Figure 8

Figure 8 Expression of *Chlorella* sp. TLD6B genes involved in the TAG biosynthesis
pathway under low (0.1 M NaCl addition, Nacl1) and high (0.8 M NaCl addition, Nacl2)
salt treatments.

(A) Expression of TPI genes; (B) Expression of GPD genes; (C) Expression of GK gene; (D)

Expression of DGAT genes. Gene IDs such as Cluster-31803.100315 are abbreviated as

Cl-3.100315. Additional abbreviated gene names are defined in Figures 3 and 6.
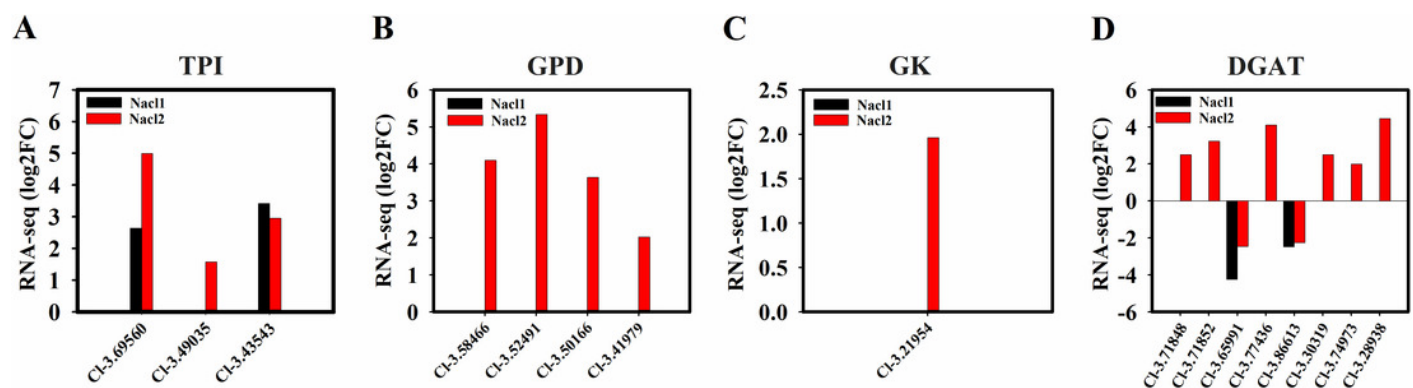
Table 1 Correlation coefficients between biomass and physiological parameters under salt stress of different durations.

*$P < 0.05$. B_6 indicates the biomass on day 6, and so forth.

1   **Table 1 Correlation coefficients between biomass and physiological parameters under salt stress of different durations.**

Biomass under different stress durations		OD$_{680}$	Carbohydrate concentration	Total lipid concentration	Adding NaCl concentration
B_6	Pearson correlation	0.822*	0.829*	0.607	−0.894
	Significance (bilateral)	0.045	0.041	0.201	0.016
B_12	Pearson correlation	0.900*	0.787	0.578	−0.736
	Significance (bilateral)	0.014	0.063	0.229	0.096
B_18	Pearson correlation	0.833*	0.905*	0.79	−0.827
	Significance (bilateral)	0.040	0.013	0.061	0.042
B_24	Pearson correlation	0.904*	0.909*	0.62	−0.935
	Significance (bilateral)	0.013	0.012	0.189	0.006

2   *$P < 0.05$. B_6 indicates the biomass on day 6, and so forth.

Table 2 Gene functional annotation.

1   **Table 2 Gene functional annotation.**

	Number of unigenes	Percentage (%)
Annotated in NR	111238	71.53
Annotated in NT	60439	38.86
Annotated in KEGG	47032	30.24
Annotated in SwissProt	84173	54.12
Annotated in PFAM	105026	67.53
Annotated in GO	109098	70.15
Annotated in KOG	51484	33.1
Annotated in all databases	23373	15.03
Annotated in at least one database	131623	84.64
Total unigenes	155503	100